Membrane-based biomolecular smart materials

2011 Smart Mater. Struct. 20 094018

(http://iopscience.iop.org/0964-1726/20/9/094018)

Smart Mater. Struct. **20** (2011) 094018 (12pp) doi:10.1088/0964-1726/20/9/094018

Membrane-based biomolecular smart materials

Stephen A Sarles and Donald J Leo

Center for Intelligent Material Systems and Structures, Mechanical Engineering Department, Virginia Tech, 310 Durham Hall, Blacksburg, VA 24061, USA

E-mail: donleo@vt.edu

Received 14 January 2011, in final form 23 March 2011
Published 30 August 2011
Online at stacks.iop.org/SMS/20/094018

Abstract
Membrane-based biomolecular materials are a new class of smart material that feature networks of artificial lipid bilayers contained within durable synthetic substrates. Bilayers contained within this modular material platform provide an environment that can be tailored to host an enormous diversity of functional biomolecules, where the functionality of the global material system depends on the type(s) and organization(s) of the biomolecules that are chosen. In this paper, we review a series of biomolecular material platforms developed recently within the Leo Group at Virginia Tech and we discuss several novel coupling mechanisms provided by these hybrid material systems. The platforms developed demonstrate that the functions of biomolecules and the properties of synthetic materials can be combined to operate in concert, and the examples provided demonstrate how the formation and properties of a lipid bilayer can respond to a variety of stimuli including mechanical forces and electric fields.

(Some figures in this article are in colour only in the electronic version)

1. Introduction

Traditional smart material systems integrate sensing, actuation, and control for the purpose of improving the functionality of a device or system. Applications that have been studied extensively include noise and vibration suppression [1, 2], shape control [3, 4], structural health monitoring [5, 6], and energy harvesting [7, 8].

One of the central components of a smart system is the material that exhibits transduction properties through coupling between multiple physical domains. Common examples of smart materials are piezoelectric materials, electrostrictive materials, shape memory alloys (SMA), and a diverse set of materials commonly referred to electroactive polymers (EAP). Piezoelectric materials, as an example, exhibit electromechanical coupling through the rotation of electric dipoles within the material [9]. Likewise, SMAs exhibit thermomechanical coupling due to a temperature-induced phase transformation [10]. Several types of EAPs exhibit transport-induced electromechanical coupling due to the existence of ionic species within the material [11–15]. In addition, multiple types of optoelectronic materials have been developed, including fiber optic sensors [16] and conducting polymers [17–19].

Over the past several years there has been significant progress in the use of biomolecules in materials for smart systems. In particular, advances in techniques to analyze, synthesize, and even genetically engineer biomolecules such as proteins [20, 21], peptides [22], and phospholipids [23, 24] has led to the ability to integrate these molecules into synthetic material platforms for the purpose of developing sensors [25, 26, 20, 27], actuators [28], and power sources [29, 30] based on the diverse functionality of biomolecules.

In the past 2 years our group has focused on the development of a class of biomolecular material systems that utilize phospholipids, peptides, and proteins as a means of introducing functionality into a diverse range of materials. Inspired by the compartmentalized structure of cells and tissues in natural systems, our work on biomolecular materials has focused on the development of cellular materials that contain physically connected compartments to allow controlled transport within the network [31–33].

Advances in the fabrication and characterization of biomolecular material systems is enabling the use of biomolecules as transducers for smart material systems. To illustrate the potential for developing new smart materials, figure 1 presents a few of the coupling properties exhibited

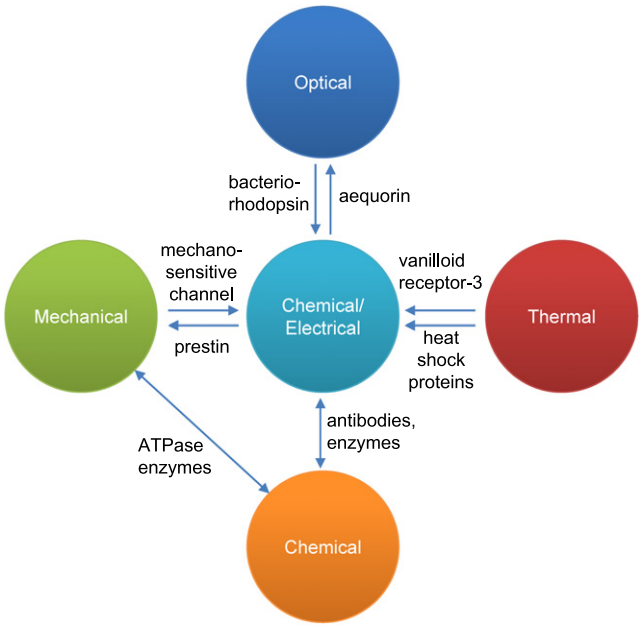

Figure 1. Representation of the coupling properties provided by natural biological molecules.

by a small set of biomolecules. The examples provided include enzymes like ATPase, which use the chemical energy in adenosine triphosphate (ATP) to produce motion [28, 35], and bacteriorhodopsin, a protein that converts the energy in photons into a proton current [27]. An important feature of this diagram is the variety of physical domains that are linked by the functions of biomolecules. This coupling map also suggests that material systems that use these elements can be designed with control over both the type and direction of energy conversion provided by biomolecules. Our work lays the foundation for the development of a wide range of stimuli-responsive materials that make use of the sheer diversity of natural and engineered biomolecules. Nonetheless, there are challenges associated with retaining the activity of these molecules in synthetic environments and constructing material systems that both enable the detection of single-molecule events and amplify these individual interactions into a global response.

The remainder of this paper is divided into two parts that highlight how our group is actively evolving membrane-based biomolecular systems into smart materials and devices by developing new methods for assembling and packaging networks of artificial cell membranes in synthetic environments. Section 2 reviews the specific systems that the Leo Group at VT has developed in the pursuit of achieving durable, packaged lipid bilayers formed at a liquid interface. Then in sections 3, 4 and 5, we demonstrate three different types of coupling mechanisms that our current platforms provide, including: mechanoelectrical coupling between the external substrate and the electrical properties (and physical structure) of a lipid bilayer, force-controlled conduction of ions through gramicidin channels in a lipid bilayer, and bioluminescent light production using controlled mixing between adjacent compartments.

2. Biomolecular material systems

Our vision of biomolecular material systems focuses on the use of biomolecules as the transduction element for devices such as sensors, actuators, and energy conversion devices. In a recent overview, the National Academy of Engineering issued a report that identified three related strategies for motivating and directing the development of biologically inspired materials: biomimicry, bioinspiration, and bioderivation [36].

The biomolecular materials studied in our work are best described by the third approach and consist of a combination of naturally occurring molecules and synthetic materials integrated to create novel multi-functional materials. Consider a material that, at the macroscopic level, consists of a synthetic matrix such as a hard or soft polymer, ceramic, or metal. Embedded within this matrix is a network of physically connected compartments that enable the transport of charge and species between individual compartments. Much like a biological material, transport between compartments can be controlled by the existence of artificial cell membranes—called lipid bilayers—formed from amphiphilic molecules that self-assemble at the interface. These selectively permeable barriers mimic the properties and functionality of the cell membrane in living systems. Also, as is the case for living systems, artificial cellular membranes can serve as scaffolds for hosting a wide range of biomolecules such as transmembrane proteins that act as channels and pumps for regulating transport between compartments.

This general form of bimolecular material system can be considered a smart material due to the stimuli-responsive properties of the network. Through previous work and our research it has been demonstrated that such a network can be made responsive to the application of a wide range of external stimuli, such as mechanical stress [37, 38], optical inputs [27], and thermal inputs [39, 40]. Likewise, it has been demonstrated that the control of collective transport across artificial membranes can produce a macroscopic pumping action and material swelling that mimics the properties of certain plant models [28, 35]. Furthermore, it has been shown through simulation that such a bimolecular material system can be used as an energy conversion device that transforms chemical energy gradients into electrical energy [29]. Thus, the embodiments studied in this work exhibit many of the same properties as other types of smart materials, but do so using functional assemblies of biomolecules. However, as a result of their makeup and bottom-up assembly, membrane-based biomolecular materials are creating a new class of multi-functional devices that can be created to function across multiple length scales.

2.1. Liquid-supported interface bilayers

The building block for our biomolecular material systems is a two-compartment network with a single lipid bilayer interface, as shown in figure 2(a). The primary components of this building block are an interior compartment containing an hydrophilic aqueous phase and an exterior region containing a hydrophobic oil phase. The interface between these two liquid phases contains amphiphilic molecules such

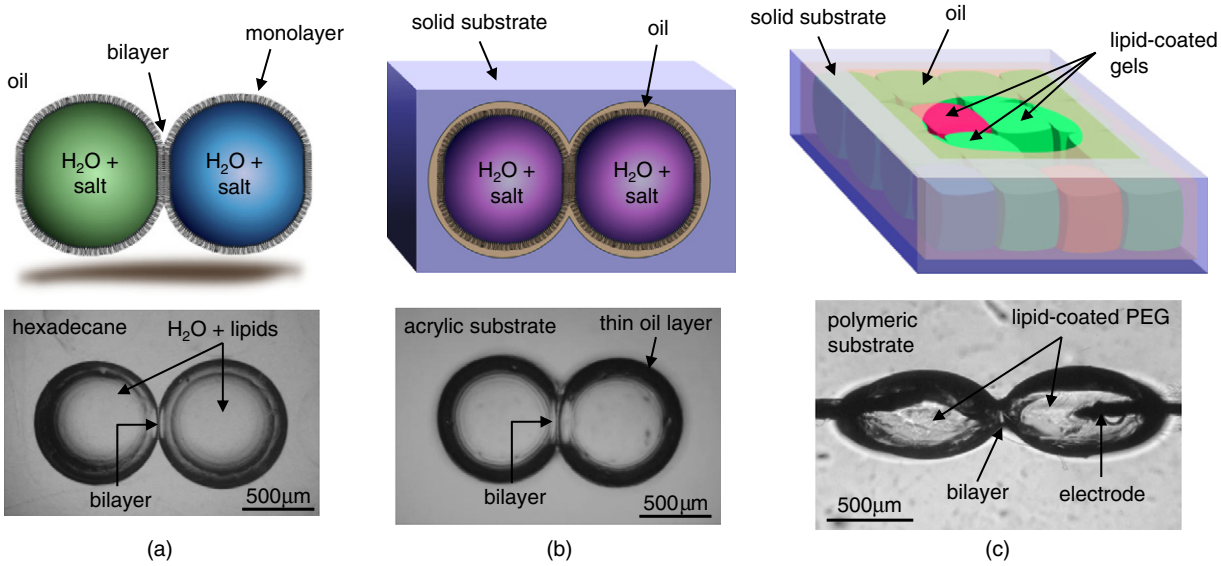

Figure 2. With physical encapsulation and the use of hydrogel aqueous compartments, the droplet interface bilayer (a) is transitioned into liquid-in-solid (b) and solid-in-solid (c) material systems, respectively.

as phospholipids or other types of surfactants that self-assemble at the hydrophilic–hydrophobic interface. A bilayer membrane consisting of two opposing amphiphilic layers forms spontaneously, stabilizing the physical interface between the two aqueous compartments upon contact. The embodiment shown in figure 2(a) was originally demonstrated by Funakoshi *et al* [41] and Holden *et al* [27] as a novel means of forming phospholipid bilayers in oil. Holden *et al* referred to the technique as the droplet interface bilayer (DIB) to differentiate it from other methods of forming supported and suspended bilayers on synthetic substrates. Holden *et al* also demonstrated that more than two lipid-coated droplets can be connected to form modular networks that feature multiple bilayer interfaces, where functional arrays are achieved by the incorporation of multiple types of biomolecules such as transmembrane proteins into each phospholipid bilayer [27, 42, 21]. And while this technique offers benefits of increased bilayer longevity and network reconfigurability, the liquid assembly formed by this approach does not immediately translate into a robust material concept.

2.2. Physically encapsulated interface bilayers

In our recent work we have evolved this embodiment to enable the formation of biomolecular networks that can be used to develop robust biomolecular material systems [32, 33]. We refer to the DIB developed by Holden *et al* [27] as a liquid-in-liquid system because the hydrophilic region is an electrolyte solution and the hydrophobic exterior is a liquid solvent. Our initial work in this field focused on demonstrating that we could encapsulate the compartments and bilayers within a solid substrate for the development of liquid-in-solid systems as shown in figure 2(b). As discussed in Sarles and Leo [32], an encapsulated liquid-in-solid system consists of an aqueous interior surrounded by a thin layer of organic solvent contained within a solid matrix with hydrophobic surface properties. This work demonstrated that physical encapsulation provides a route for obtaining more portable assemblies that are capable of withstanding several *g*s of mechanical vibration and impact loads. Sarles and Leo have also developed a means for forming phospholipid bilayers within solid substrates by the application of a controlled mechanical force [33]. The technique, denoted the regulated attachment method (RAM), involves the application of a mechanical force such that the aperture between two compartments is reduced in size until the aqueous fluid within the compartments separates into two volumes (see figure 3). Following separation, each aqueous volume then becomes fully encased in a lipid monolayer as phospholipids contained in either liquid phase self-assemble at the hydrophilic–hydrophobic interface. Relaxation of the mechanical force brings the two monolayers into contact, such that interactions between the two monolayers expel the hydrophobic fluid between the monolayers, resulting in the formation of a bilayer membrane at the interface [43].

2.3. Solidified biomolecular assemblies

Most recently our work has focused on the evolution of this technology into solid-in-solid systems that more closely resemble a monolithic biomolecular material. Sarles and Leo recently demonstrated that a hydrophilic gel can be substituted for the aqueous electrolyte and the hybrid material retains all of its properties associated with bilayer stability and bilayer formation [34]. As depicted in figure 2(c), the solid-in-solid embodiment features solid interior compartments (or cells) surrounded by a thin fluid layer that supports the amphiphilic molecules at the hydrophilic–hydrophobic interface. Both the solid compartments and the hydrophobic fluid are housed in a outer solid substrate. As discussed in Sarles and Leo [34], the solidified interior compartment can consist of materials such polyethylene glycol (PEG) hydrogels of varying weight

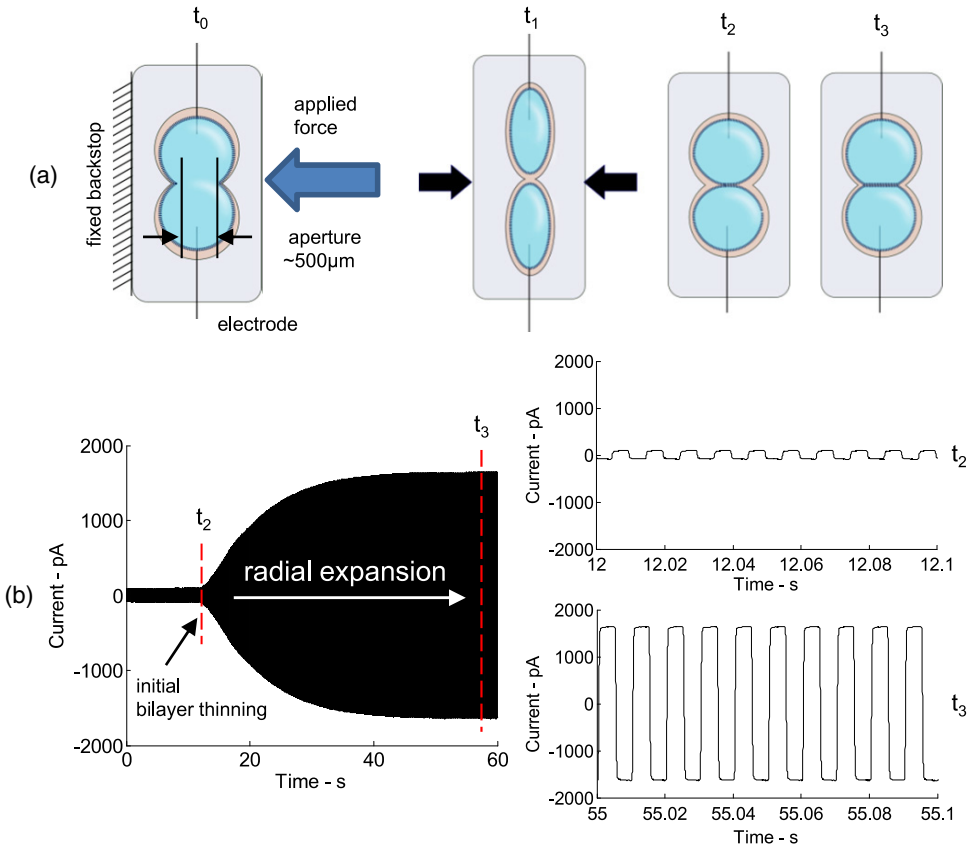

Figure 3. The regulated attachment method (RAM) enables the formation of an interface bilayer within flexible substrates by using a mechanical force to first separate and then reconnected lipid-coated aqueous volumes. A top view of the flexible PDMS substrate shows how the conductive aqueous phase (t_0) is separated at t_1 and then reconnected to from a bilayer at t_2. The established bilayer interface is capacitive, as shown by the square-wave current produced by an applied triangular voltage waveform, and expands in area to an equilibrium state at t_3.

percentage to enable the formation of solidified, yet water-swollen, interiors that exhibit a range of mechanical properties. When using PEG, the gelation process can be controlled by the introduction of a UV-curable initiator within the gel, although other means of curing the gel (e.g. temperature control) could also be used. Experiments confirmed the ability to use the regulated attachment method to control bilayer formation within solid-in-solid systems and the resulting membranes were shown to demonstrate considerable resistance to rupture during simple drop tests [34].

This particular embodiment provides a new range of possibilities in constructing biomolecular material systems, since now the aqueous phase takes on the shape of the gel structure. In this manner, non-spherical gels are possible (unlike with DIBs) and gel structures can be physically anchored to the substrate for additional support or for stability during fabrication.

3. Electromechanical properties of membrane-based biomolecular material systems

Many applications of smart materials rely on the use of materials that exhibit electromechanical (or mechanoelectrical) coupling, such as piezoelectric materials, electrostrictive materials, or EAPs. We have utilized the fabrication methods introduced in section 2.3 and detailed in several publications [32–34] to develop a building block for biomolecular material systems that consists of a two-compartment, single-interface system that exhibits mechanoelectrical coupling due to the existence of a phospholipid bilayer membrane at the interface (see figure 3).

3.1. Mechanically activated conductor-to-insulator transitions

In biological systems, membranes formed from amphiphilic molecules such as phospholipids serve as barriers to ion transport. As such, they are good insulators to charge motion and produce very high levels of electrical insulation in conducting media. Previous works to characterize lipid bilayers have shown that these thin membranes have electrical resistances as high as 10–100 MΩ cm^2 and exhibit a capacitance of 0.1–1.0 μF cm^{-2} due to the dielectric nature of the hydrophobic interior of the membrane [44–50].

In its simplest form, the regulated attachment method for forming bilayers within solid substrates enables the development of biomolecular materials that exhibit controllable transitions between insulating and conducting states. Consider the building block shown in figure 3(a) prior to the existence of the bilayer membrane at the interface between the two compartments. In this state the electrical properties of the material are dependent on the conduction of ionic species

through the hydrophilic media (either a liquid salt or a hydrogel) when a potential is applied at the electrodes. While it is well established that changing the salt concentration in the conducting media can vary the conductivity, the RAM technique enables much larger, reversible changes in conductivity by altering the physical location and organization of phospholipid molecules contained in the liquid phase.

To demonstrate this concept, experiments were performed to quantify the relationship between an applied mechanical load and the ionic conductivity of the building block (figure 3). The aqueous volumes used in this test were 200 nl of 2 mg ml^{-1} diphytanoyl phosphatidylcholine (DPhPC) phospholipid vesicles (purchased as lyophilized powder, Avanti Polar Lipids, Inc.) suspended in 500 mM KCl (Sigma), 10 mM MOPS (Sigma), pH 7 buffer solution and hexadecane (Sigma), used as the oil phase. The flexible substrate was fabricated from Sylgard 184 polydimethyl siloxane (Dow Corning). Mechanical loads are applied using a displacement-controlled micromanipulator in the fixture shown in figure 3(a).

The building block is initially in a conducting state at t_0 with no bilayer present between the compartments. In this configuration the two compartments form a single conducting medium whose ionic transport properties are a function of the concentration of the aqueous salt solution. Upon application of a mechanical load the substrate begins to deform and causes the aperture between the compartments to become smaller. At t_1 the single volume separates into two separate volumes due to ingress of the non-conducting organic phase that surrounds the aqueous compartments. At this time the electrical current drops to approximately zero due to the fact that an open circuit occurs between the two electrodes. Measurements of the current in this configuration are approximately equal to the noise level of the measurement device. During the time that the aqueous media in the compartments are separated, phospholipid molecules self-assemble at the interface between the hydrophobic solvent and the aqueous salt. Upon relaxation of the mechanical load, the two aqueous volumes are brought back into contact and the monolayers that have formed at the boundaries of the separate droplets form a phospholipid bilayer at the interface between the two compartments.

Bilayer formation is observed by applying a small oscillating potential across the interface and measuring the current induced across the bilayer. Due to the capacitive nature of the bilayer, an applied potential with a triangular waveform will produce a square-wave signal in the current whose amplitude is proportional to the capacitance of the bilayer. As shown in figure 3(b), the formation of the bilayer can be measured by the growth of the current amplitude as a function of time. We denote the beginning and the end of this process as t_2 and t_3, respectively.

At the end of the mechanical loading cycle the electrical properties of the building block have transformed from conducting to near insulating. Measurements of the electrical impedance across the aperture before and after mechanical loading confirm a 10^4-fold decrease in the low-frequency conductance across the interface (figure 4). The admittance measurement also quantifies the capacitance of the bilayer which, as will be discussed in section 3.2, can be used to measure the size of the bilayer.

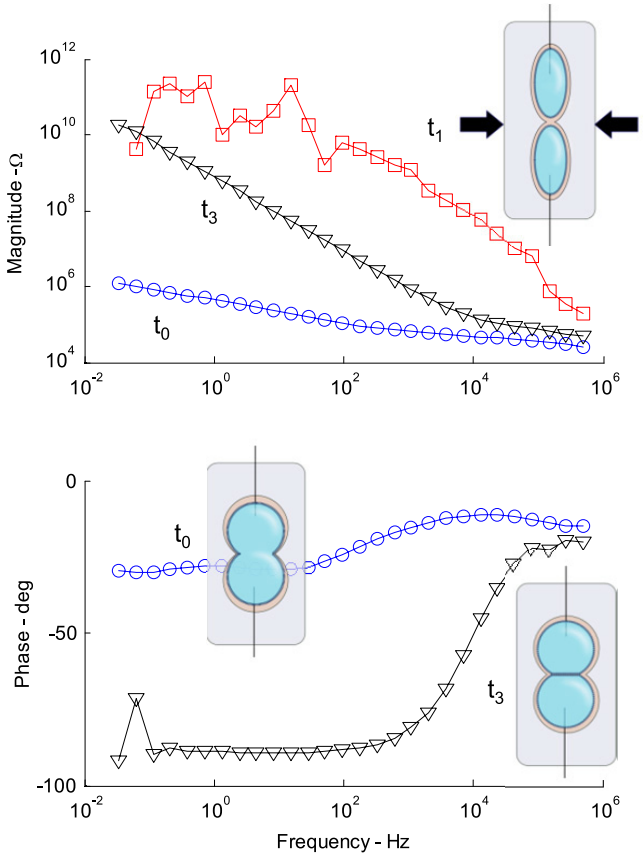

Figure 4. Electrical impedance spectroscopy measurements confirm that the applied force separates the conducting volume at t_1 and that the assembled bilayer interface at t_3 is much less conductive than the initial aqueous solution, t_0. The phase measurement for the separated aqueous volumes (t_1) is not shown due to the noisy nature of this open-circuit measurement.

As noted earlier, this electrical transition is a reversible process. The material system resumes its original conductive state (i.e. t_0) upon induced bilayer rupture since the stability of the membrane has both mechanical and electrical limits [31].

3.2. Force-induced changes in membrane capacitance

In addition to forming barriers to ion transport, the bilayer acts as an electrical capacitor, where the nominal capacitance is directly proportional to the area of the interface. For example the specific capacitance of a phosphatidylcholine (PC) lipid bilayer is approximately 0.6 μF cm^{-2} [51, 27], which when inverted results in a specific area (i.e. area per unit capacitance) of 167 μm^2 pF^{-1}. To assist in visualizing the size of the bilayer, we can also define an effective circular diameter as the diameter of a circular membrane of equal area. Using the accepted value for specific capacitance of 0.6 μF cm^{-2}, the effective circular diameter of a bilayer membrane per square root of the capacitance is 14.6 μm pF$^{-1/2}$. Thus, by measuring the capacitance of the bilayer in real time we can estimate the bilayer area and effective circular diameter.

With RAM, not only can a bilayer be formed to change the conductivity of the material, but the size of the interface can be controlled by displacement of substrate caused by an applied

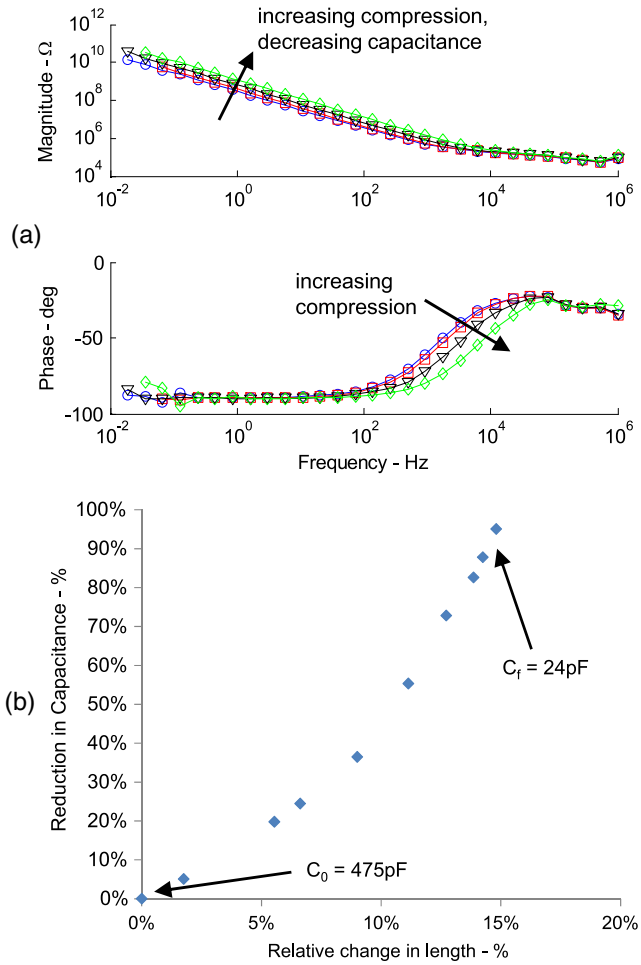

Figure 5. EIS measurements illustrate how forces applied to the substrate produce electrical changes in the impedance of the interface (a). The capacitance (area) of the bilayer decreases as the force applied to the substrate is increased (b). A compression force of approximately 1280g is required to produce a 15% change in length for the PDMS substrate used in this experiment.

mechanical force [33]. While others have used electric fields to increase the size of the interface [52], the RAM technique demonstrates that a mechanical stimulus can be used to enable both increases and decreases in the size of the bilayer. As a result, the measured capacitance of the bilayer contained in the substrate correlates directly to the applied load on the outer material (figure 5).

Electrical impedance spectroscopy (EIS) measurements across the bilayer at each compression level show that an increasing force causes the capacitance of the bilayer to change and the impedance magnitude to increase at frequencies below approximately 1 kHz (figure 5). Initially the bilayer has a capacitance of 475 pF prior to compression of the substrate. As the force is slowly increased the substrate deforms, and deformation of the substrate and its internal compartments causes the two volumes to be pulled apart slightly. Dimensional change of interface causes a reduction in the size of the bilayer, which can be measured as a variation in the bilayer capacitance. Figure 5(b) illustrates that changes in substrate length of the order of 0–15% cause large reductions in the capacitance. This range of deformation corresponds to an applied force of 0–1280g for the PDMS substrate used in this test and causes the capacitance of the membrane to decrease by a factor of nearly 20-fold from 475 pF to a minimum value of 24 pF. This change in capacitance is equivalent to a change in effective circular diameter from 318 to 72 μm. The application of an additional force causes the two volumes to completely separate, thus eliminating the capacitive effects of the bilayer.

Our experiments have also demonstrated that the mechanoelectrical coupling properties of the building block are reversible. Though not shown in figure 5, the size of the interface grows back to its initial state as the compression force is removed and the adjacent lipid-coated volumes are allowed to have increased contact [33]. We anticipate that an even higher sensitivity (change in capacitance per force applied) and a larger number of bilayer interfaces could be realized with simple modifications to the substrate design.

The sensitivity of the capacitance change per force applied can also be controlled by changing the oil (solvent) used in this system. In general, smaller-molecule solvents such as decane lead to greater oil retention in the membrane and a smaller area of contact between two lipid encased aqueous volumes due to an increase in the bulk interfacial tension of the monolayers [43]. On the other hand, larger-molecule solvents, such as squalene, produce thinner, more-'solvent-free' membranes (with higher specific capacitances) due to lower oil retention in the bilayer and an increased interface area caused by reduced monolayer surface tension [49, 43]. Based on capacitance alone, this trend suggests that a 'solvent-free' membrane may provide a larger change in the capacitance of the interface per unit applied force compared to a less-capacitive membrane that contains some solvent. However, our own experiences have also shown that smaller interfaces formed with either decane or hexadecane are more stable under mechanical vibrations, despite having a decreased free energy of thinning (a measure of the thermodynamic stability of the interface) [43] and retaining a greater amount of oil in the bilayer (which can negatively affect the functions of transmembrane proteins [49, 53]). In this work, hexadecane is used as the oil phase for all studies.

4. Mechanosensitive biomolecular transduction

In addition to an electromechanical coupling between the electrical characteristics (and physical structure) of the bilayer and an applied mechanical force to the outer substrate, mechanical forces on the outer surface of the biomolecular material system can also affect how other biomolecules incorporated into the bilayer enable transport from one aqueous compartment to the next. This form of coupling between the external synthetic material and the internal biomolecular assembly is the product of the hybrid construction of the material system and is unique to the biomolecular materials developed within our group.

In order to demonstrate mechanosensitive conduction across a bilayer, we performed a series of experiments in which gramicidin peptides (a mixture of antibiotic compounds, gramicidin A, B and C purchased from Sigma) were

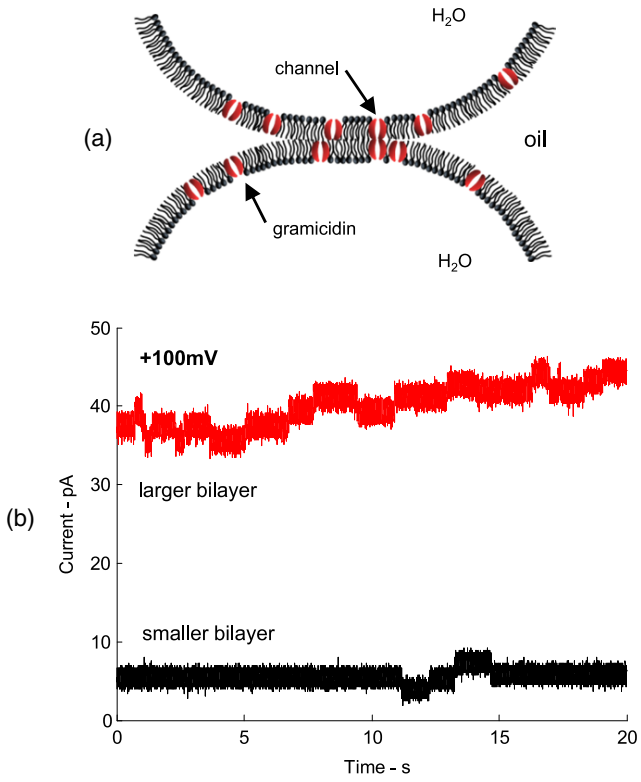

Figure 6. A small number of gramicidin peptides in the bilayer (a) exhibit discrete changes in the conductance of the membrane at a given voltage level, where the frequency and average number of aligned gramicidin channels for a fixed peptide concentration depends directly on the area of the bilayer (b). Note that the magnitude of the change in current is dependent on the conductance of a given channel—related to both the physical size of the channel and the conductivity of the aqueous solution—and the applied voltage.

incorporated into the lipid membrane. The RAM is used to initiate bilayer formation within a polyurethane substrate (PU; ClearFlex 50, Smooth-On, Inc.) that features the same compartment geometry discussed in section 3 [33]. Gramicidin peptides are small molecules that span half the thickness of the bilayer. A conductive pathway through the membrane, called an ion channel, is formed when gramicidin molecules in both halves of the bilayer momentarily align [54, 55, 41, 53] (see figure 6(a)). Since the insertion and transient alignment of peptides to form conductive ion channels are probabilistic in nature, the average conductance of a bilayer containing gramicidin channels depends on both the number of peptides added to each aqueous volume and the effective area of the bilayer. Therefore, in this example, the conductance of the membrane (e.g. the number of ions that can flow through the gramicidin channels) is regulated by the application of a mechanical force to control bilayer area for a given concentration of gramicidin in solution.

Figure 6(b) presents experimental data collected on a single interface formed between aqueous compartments that contain gramicidin peptides in addition to lipid vesicles and salt. The channels self-assemble into the interface and their alignment is measured as an increase in the current that flows through the membrane. At low gramicidin concentrations (5 ng ml^{-1} added to the lipid vesicle solution), a limited number of gramicidin channels exist in each leaflet of the membrane and the effective bilayer conductance is still quite low. The two current traces illustrate how the current at a steady transmembrane voltage of 100 mV changes discretely [in increments of 1.5–2.0 pA (15–20 pS) [54, 41]] as gramicidin molecules momentarily connect and disperse.

Furthermore, these traces demonstrate two effects of increasing the size of the bilayer on the measured current: increased frequency of discrete current transitions and increased average current. When the membrane is small (the applied force is large), the presence of only a few channels produces a small average current and the frequency of channel association (and disassociation) is low. When the force applied to the substrate is reduced, however, the bilayer adopts a larger interfacial area, allowing more gramicidin channels to reside in the membrane. The increased number of channels present in the membrane causes the average current to increase and also the frequency of gramicidin gating events to increase (figure 6(b)).

This coupling between the external mechanical force and the internal conductance is magnified when the concentration of gramicidin added to each aqueous compartment is increased. In a second set of tests, a new interface is formed between aqueous volumes containing 500 ng ml^{-1} gramicidin peptides in the lipid vesicle solution. The force applied to the substrate is incrementally increased, and at each force level cyclic voltammetry (CV) and EIS measurements are performed to obtain the current–voltage relationship and the resistance and capacitance of the bilayer, respectively. These data are shown in figure 7.

The linear relationship between current and voltage show that the conductance of gramicidin channels does not depend on the applied voltage, while the magnitudes of the measured currents confirm that with more channels present in the bilayer the amount of current that flows through the membrane rises substantially (figure 7(a)). Whereas the average current at 100 mV for 5 ng ml^{-1} gramicidin was only 10–50 pA, 500 ng ml^{-1} gramicidin in the solution yields currents of the order of 100 pA–1 nA. The different traces represent measurements of current through the bilayer for the different forces applied to the substrate. For zero compression force and a large interface, the slope of the current–voltage curve (e.g. the effective conductance of the membrane) is quite steep (0.0085 nA mV^{-1}, 8.5 nS). However, when the force is high (nearly 1500g) and the membrane is small, this slope decreases by a factor of 7–0.0013 nA mV^{-1} (1.3 nS), since fewer aligned channels are present to allow for ion flow. The symmetry of the traces with respect to the polarity of the voltage shows that gramicidin channels permeabilize the membrane to ion flow in both directions equally.

In order to demonstrate that the number of ion channels in the bilayer does decrease as the force is increased, the nominal resistance and specific membrane resistance (per the area of the bilayer) versus the change in length of the substrate are compared in figure 7(b). Consistent with the decrease in membrane conductance observed in the current–voltage traces, EIS measurements confirm that the nominal resistance

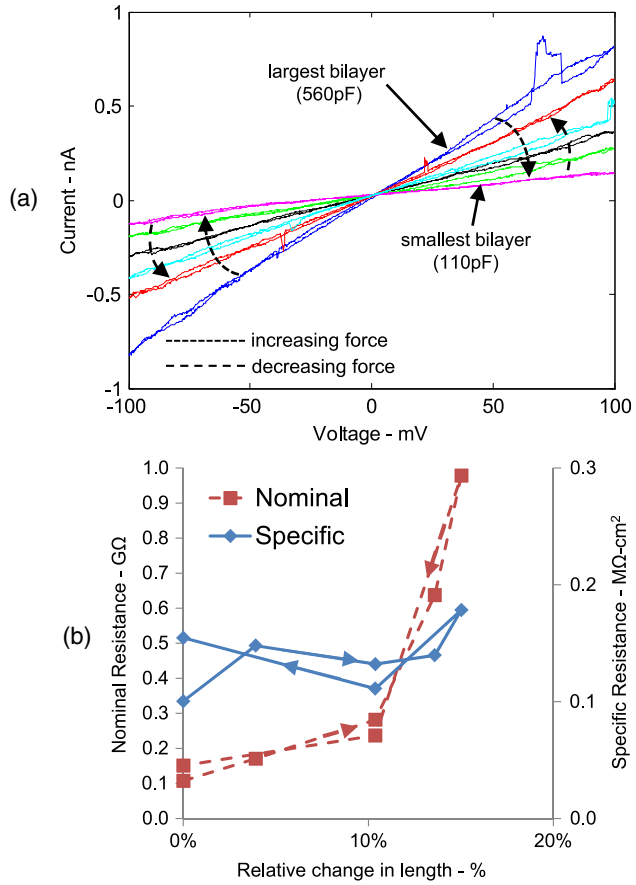

Figure 7. At higher concentrations of gramicidin in the bilayer, the applied force on the substrate produces changes in nominal resistance of the membrane (a). The arrows in the data series lines in (b) show the direction of the change in compression. These tests are performed using a PU substrate, which requires approximately 1470g to compress the overall length by 15%.

of the membrane increases by nearly a factor of 10 for the range of forces applied to the material. However, the specific membrane resistance computed using the measured nominal resistance and the area of the membrane obtained from the measured capacitance do not change by the same amount. Instead, the specific membrane resistance remains between roughly 0.1 and 0.2 MΩ cm^2 for all compression levels. These data indicate that the relative number of gramicidin peptides contained in both lipid monolayers (and the relative number of channels per unit area of the bilayer) does not vary drastically during the experiment. As a result, the nominal resistance of the membrane can be regulated in both directions by merely controlling the size of the interface, where the reversibility of the nominal membrane resistance is attributed to the fact that gramicidin peptides can link together as the opposing monolayers form a thinned interface and then readily separate as the monolayers are unzipped by compression of the substrate.

This example demonstrates that deformations of the surrounding substrate can also be used to control the effect of other types of biomolecules contained in the bilayer—here, the incorporation of gramicidin channels in the interface was used to translate an external force into a measurable change in the current through the membrane. One challenge in prescribing consistent transduction sensitivity is maintaining the concentration of ion channels held in the bilayer. Since our characterization took place within 1 h of bilayer formation, the long term behavior of this transducer was not studied. However, our results for two different gramicidin concentrations suggest that the average number of channels contained in the bilayer upon saturation can be regulated by controlling the concentration of gramicidin in each aqueous volume (see figures 6 and 7).

5. Biofunctional compartments

Functionality in biomolecular material systems can also result from the contents of specific compartments in the network. Whereas the previous two examples demonstrated that the functionality of the biomolecular system can be tailored by the properties of the bilayer membrane, we can also demonstrate that the functionality can be controlled by tailoring the contents of the compartments themselves. Specifically, we demonstrate that each compartment can be used to contain a given substance and that the bilayer formed between adjacent compartments can be used to selectively control the interaction of these species. The example that is described involves a chemical reaction, where the two reactants are stored in separated aqueous volumes on either side of the bilayer. By controlling the formation and rupture of the bilayer, the reaction can be initiated in a controlled manner. Furthermore, we discuss how the use of biomolecules in the bilayer may also provide a mechanism for regulating the transport of reactants from one side of the bilayer to other.

We performed a series of experiments in a rigid acrylic substrate with two aqueous compartments (200 nl each) in which one compartment contains calcium ions (100 mM) and the second compartment contains 10 mg ml^{-1} of aequorin (Toy Grade, 50% purity, Nanolight Technologies), a calcium-activated photoprotein found in the *Aequorea victoria* species of jellyfish (figure 8(a)). In nature, jellyfish use aequorin to bioluminesce with blue light (465 nm), a process well characterized by Shimomura [56, 57] and one that eventually led to the understanding and wide-spread use of green fluorescent protein (GFP) in biological and biomedical imaging [58]. In this section, we show that the same reaction can be performed in biomolecular material systems to demonstrate light production and color change. Both aqueous compartments also contain phospholipids necessary for monolayer self-assembly and bilayer formation. Digital images of artificial bioluminescence generated by rupture of the bilayer that separates the compartments were collected in dark room conditions every 0.25 s using a Canon G6 digital camera connected to the objective lens (5×) of a Zeiss AxioVert 40CFL inverted microscope.

With a lipid bilayer to separate the reactants in both compartments, the first frame in figure 8(b) shows that the connected aqueous volumes do not produce any blue light. However, when the interface is ruptured (in this case a mobile electrode attached to a motorized manipulator was used to mechanically rupture the interface), the contents of the two

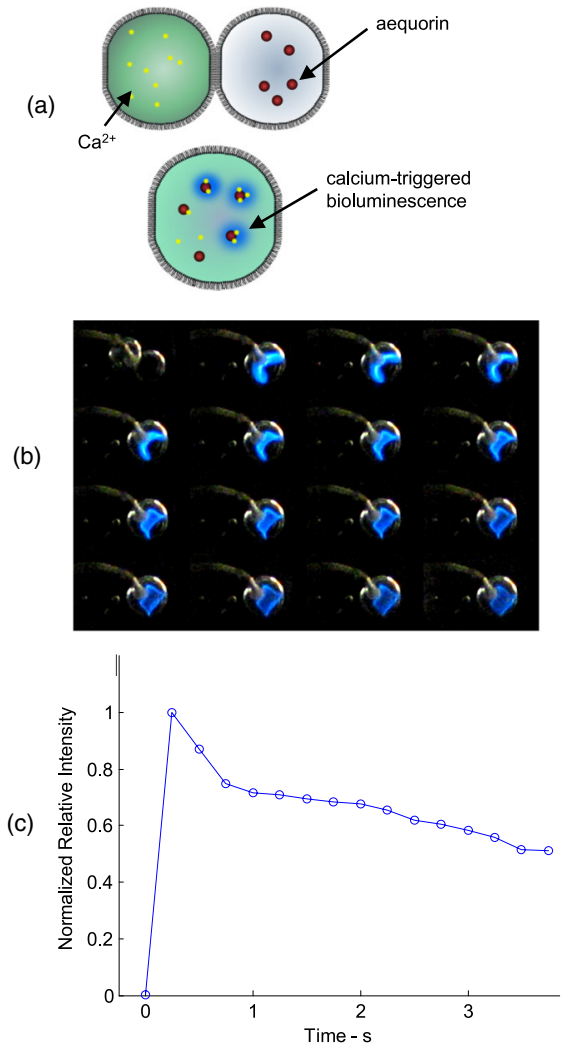

Figure 8. (a) A schematic of the two-compartment system shows how bioluminescence is triggered by the rupturing of the bilayer interface that separates the calcium- and aequorin-containing compartments. Burst images collected every 0.25 s show the bioluminescence produced calcium-activated aequorin contained in artificial biomolecular compartments (b). A measure of the light produced during each frame in (b) plotted versus time (c).

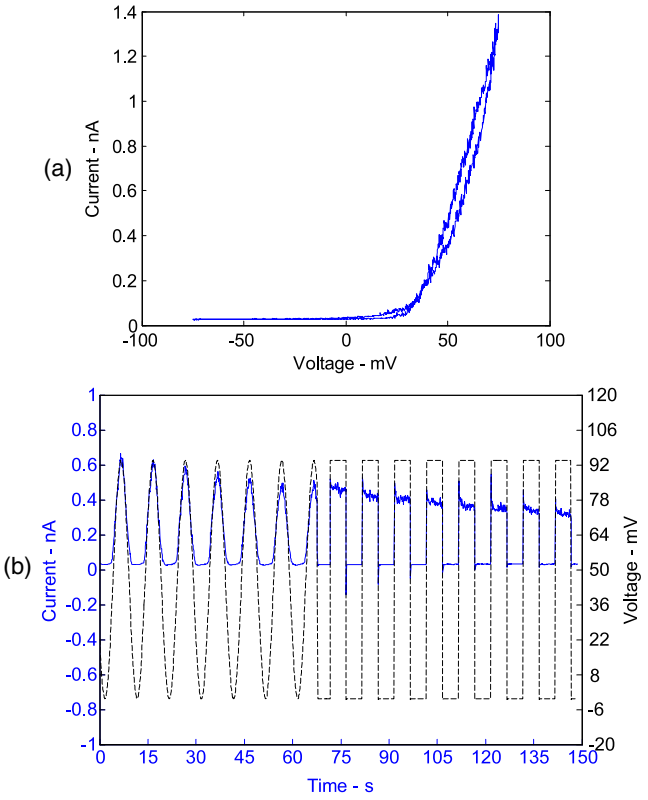

Figure 9. The current–voltage relationship of a lipid bilayer containing alamethicin peptides added to one compartment at a concentration of 10 mg ml^{-1} (a) and the rectified current flow (solid) per oscillating membrane voltage (dashed) for different waveforms (b).

volumes mix and blue light is emitted as calcium ions bind to aequorin molecules suspended in the aqueous interior of the volume. The frames in this image show that the intensity of the light grows rapidly after coalescence and then fades slowly over the next several seconds. The images also show that the area of light emission expands due to the diffusion of calcium ions to unactivated aequorin molecules contained in the volume.

A plot of the normalized relative intensity of blue light—defined as the sum of the intensities of all blue pixels—produced in each frame is plotted in figure 8(c). The first data point represents the two-compartment system prior to bilayer rupture. The rapid rise to the second data point, the maximum intensity measured, demonstrates that the activation time for aequorin is much less than 0.25 s [56]. Subsequent intensity values decrease at a much slower rate, a process balanced by the rate at which light produced by activated aequorin molecules fades and the diffusion of unbound calcium ions to previously unactivated aequorin molecules in solution. Per the 2 μg of aequorin contained in this volume and a luminescence activity of 4×10^{15} photons mg^{-1} for aequorin [59], we estimate that the reaction is capable of emitting 8×10^{12} photons in total and producing blue light for approximately 5–6 s.

In addition to bilayer rupture (either by mechanical or electrical [31] means), controlling the rate of reaction between aequorin molecules and calcium ions can also be done by using ion channels in the bilayer. For example, a voltage-gated ion channel such as alamethicin can be used to meter the flow of calcium ions in order to trigger light emission by controlling the applied voltage across the bilayer. Figure 9(a) presents the current–voltage relationship for a bilayer containing alamethicin ion channels oriented in the membrane in only one direction (the direction of self-insertion is controlled by which aqueous compartment contains the peptides). Alamethicin peptides aggregate in the membrane and form open, conductive channels upon the application of a voltage [60–62]—this activity as shown by the current–voltage characteristic is very much like that of a diode. At transmembrane voltages above 50–70 mV, the conductivity of the membrane (the slope of the current–voltage curve) increases by three orders of magnitude, from an off-state resistance at 0 mV of 41 GΩ to an on-state resistance at 60 mV of 29 MΩ. While not shown in this data, a symmetric

diode-like behavior at both polarities occurs when alamethicin channels are oriented in the membrane in both directions [63].

Thus, the transport of one type of ion from one side of the membrane to the other can be controlled with the applied voltage across the bilayer. Figure 9(b) demonstrates half-wave rectification of calcium ion transport using alamethicin channels for both sinusoidal and square-wave applied voltages. These data demonstrate that the rate of reactions can be precisely controlled using biomolecules. Unfortunately, in the case of bioluminescence using aequorin, reducing the rate of ion flow significantly reduces the intensity of the emitted light; therefore, no images were obtained during alamethicin-controlled transport. Nevertheless, this example highlights that the functionality of biomolecules can be combined in biomolecular systems, in many cases regardless of the origin of the biomolecules that are used. Here, alamethicin peptides from a fungus are combined with synthetic phospholipids and photoproteins from jellyfish to create a collective utility between an applied voltage and the resulting light production resulting from regulated transport into specific aqueous compartments.

Assigning functionality to specific building blocks is motivated by the varying contents and tasks performed in the different compartments of living cells. In this example, we used a naturally occurring photoprotein called aequorin to demonstrate that the contents of specific compartments can also demonstrate coupling between different modes of energy. It is important to remember that this approach for creating functional material systems is not limited to biomolecules. Our recent work with polymeric hydrogel volumes shows that synthetic materials can be incorporated into these volumes, where the composition and material properties of the gel expand the uses for and responses from these volumes, including: immobilizing enzymes and facilitating controlled release of chemical species [64], exhibiting mechanical actuation due to changes in pH or temperature [65, 64], and even producing light or changing color due to electrical potentials [66, 67] and temperature [68].

6. Summary and conclusions

In this work we demonstrated that biomolecular systems that incorporate lipid bilayer membranes can be tailored to produce a range of stimuli-responsive behavior. Electromechanical coupling can be introduced by tailoring the properties of the lipid bilayer. Static measurements were performed to demonstrate that the capacitance of the bilayer can be correlated to the applied deformation of the surrounding substrate. We also demonstrated that the incorporation of peptides within the bilayer can introduce stimuli-responsive behavior that couples the conductance of the membrane to the applied load. Finally, we demonstrated that bioluminescence could be produced by the controlled mixing of the contents of the individual compartments contained within the substrate. By rupturing the membrane either mechanically or electrically, we can control the illumination of the material over a time span of several seconds. A key advance that enables this functionality is the transition of liquid-in-liquid molecular assemblies into solid-in-solid hybrid material systems. Through encapsulation, an internal network of compartments can be assembled, connected, and solidified to produce aqueous compartments separated by lipid bilayers. Unlike other smart materials, this approach yields a material platform in which many different (and multiple) types of coupling can be designed into one network. The various examples highlighted in this paper specifically demonstrated that these forms of coupling can occur as a result of the biomolecules themselves or due to interactions between the biomolecular assemblies and the outer solid substrate.

It is interesting to note that these processes work at length scales and power levels associated with biological systems. The membrane itself is on the order of 5 nm thick and the current levels produced by ion transport are on the order of 1–100 pA. The fact that the functional element of our building blocks is at the nanoscale provides evidence that the materials could be significantly reduced in size. Also, the power levels associated with the passage of the current are of the order of fW to pW, making it possible to operate these material systems at very low energy levels.

Acknowledgments

Financial support for this work was provided by the Office of Naval Research (N000140810654) and the National Science Foundation Grant EFRI-0938043.

References

[1] Benjeddou A 2001 Advances in hybrid active–passive vibration and noise control via piezoelectric and viscoelastic constrained layer treatments *J. Vib. Control* **7** 565–602
[2] Hagood N W and von Flotow A 1991 Damping of structural vibrations with piezoelectric materials and passive electrical networks *J. Sound Vib.* **146** 243–68
[3] Chaudhry Z and Rogers C A 1991 Bending and shape control of beams using SMA actuators *J. Intell. Mater. Syst. Struct.* **2** 581–602
[4] Bilgen O, Erturk A and Inman D J 2010 Analytical and experimental characterization of macro-fiber composite actuated thin clamped-free unimorph benders *J. Vib. Acoust.* **132** 051005
[5] Park G, Cudney H H and Inman D J 2000 Impedance-based health monitoring of civil structural components *J. Infrastruct. Syst.* **6** 153–60
[6] Park G, Sohn H, Farrar C R and Inman D J 2003 Overview of piezoelectric impedance-based health monitoring and path forward *Shock Vib. Dig.* **35** 451–63
[7] Sodano H A, Inman D J and Park G 2004 A review of power harvesting from vibration using piezoelectric materials *Shock Vib. Dig.* **36** 197–205
[8] Anton S R and Sodano H A 2007 A review of power harvesting using piezoelectric materials 2003–2006 *Smart Mater. Struct.* **16** R1
[9] Berlincourt D A 1964 Piezoelectric and piezomagnetic materials and their function in transducers *Phys. Acoust.* **1** 169
[10] Boyd J G and Lagoudas D C 1996 A thermodynamical constitutive model for shape memory materials. part I. The monolithic shape memory alloy *Int. J. Plast.* **12** 805–42
[11] Madden J D, Cush R A, Kanigan T S and Hunter I W 2000 Fast contracting polypyrrole actuators *Synth. Met.* **113** 185–92

[12] Spinks G M, Liu L, Wallace G G and Zhou D 2002 Strain response from polypyrrole actuators under load *Adv. Funct. Mater.* **12** 437–40
[13] Tadesse Y *et al* 2008 Polypyrrolepolyvinylidene difluoride composite stripe and zigzag actuators for use in facial robotics *Smart Mater. Struct.* **17** 025001
[14] Shahinpoor M *et al* 1998 Ionic polymer–metal composites (ipmcs) as biomimetic sensors, actuators and artificial muscles—a review *Smart Mater. Struct.* **7** R15
[15] Akle B J, Bennett M D and Leo D J 2006 High-strain ionomeric-ionic liquid electroactive actuators *Sensors Actuators* A **126** 173–81
[16] Udd E 1995 An overview of fiber-optic sensors *Rev. Sci. Instrum.* **66** 4015–30
[17] Sirringhaus H, Tessler N and Friend R H 1998 Integrated optoelectronic devices based on conjugated polymers *Science* **280** 1741–4
[18] Ho P K H, Thomas D S, Friend R H and Tessler N 1999 All-polymer optoelectronic devices *Science* **285** 233–6
[19] Bisi O, Ossicini S and Pavesi L 2000 Porous silicon: a quantum sponge structure for silicon based optoelectronics *Surf. Sci. Rep.* **38** 1–126
[20] Guan X, Gu L-Q, Cheley S, Braha O and Bayley H 2005 Stochastic sensing of tnt with a genetically engineered pore *ChemBioChem* **6** 1875–81
[21] Maglia G, Heron A J, Hwang W L, Holden M A, Mikhailova E, Li Q, Cheley S and Bayley H 2009 Droplet networks with incorporated protein diodes show collective properties *Nat. Nano* **4** 437–40
[22] Walker B, Braha O, Cheley S and Bayley H 1995 An intermediate in the assembly of a pore-forming protein trapped with a genetically-engineered switch *Chem. Biol.* **2** 99–105
[23] Sun X-L, Cui W, Kai T and Chaikof E L 2004 A facile synthesis of bifunctional phospholipids for biomimetic membrane engineering *Tetrahedron* **60** 11765–70
[24] Wong D, Jeon T-J and Schmidt J 2006 Single molecule measurements of channel proteins incorporated into biomimetic polymer membranes *Nanotechnology* **17** 3710
[25] Sackmann E 1996 Supported membranes: scientific and practical applications *Science* **271** 43–8
[26] Bayley H and Cremer P S 2001 Stochastic sensors inspired by biology *Nature* **413** 226–30
[27] Holden M A, Needham D and Bayley H 2007 Functional bionetworks from nanoliter water droplets *J. Am. Chem. Soc.* **129** 8650–5
[28] Sundaresan V B, Homison C, Weiland L M and Leo D J 2007 Biological transport processes for microhydraulic actuation *Sensors Actuators* B **123** 685–95
[29] Xu J, Sigworth F J and LaVan D A 2009 Synthetic protocells to mimic and test cell function *Adv. Mater.* **22** 120–7
[30] Sundaresan V B and Leo D J 2010 Chemoelectrical energy conversion of adenosine triphosphate using atpases *J. Intell. Mater. Syst. Struct.* **21** 201–12
[31] Sarles S A and Leo D J 2009 Tailored current–voltage relationships of droplet–interface bilayers using biomolecules and external feedback control *J. Intell. Mater. Syst. Struct.* **20** 1233–47
[32] Sarles S A and Leo D J 2010 Physical encapsulation of droplet interface bilayers for durable, portable biomolecular networks *Lab Chip* **10** 710–7
[33] Sarles S A and Leo D J 2010 Regulated attachment method for reconstituting lipid bilayers of prescribed size within flexible substrates *Anal. Chem.* **82** 959–66
[34] Sarles S A, Justin Stiltner L, Williams C B and Leo D J 2010 Bilayer formation between lipid-encased hydrogels contained in solid substrates *ACS Appl. Mater. Interfaces* **2** 3654–63
[35] Sundaresan V B and Leo D J 2008 Modeling and characterization of a chemomechanical actuator using protein transporter *Sensors Actuators* B **131** 384–93
[36] Materials National Research Council. Committee on Biomolecular and Processes *Inspired by biology: From Molecules to Materials to Machines* 2008 (Washington, DC: National Academies Press)
[37] Sukharev S I, Blount P, Martinac B, Blattner F R and Kung C 1994 A large-conductance mechanosensitive channel in e. coli encoded by mscl alone *Nature* **368** 265–8
[38] Gil Z, Silberberg S D and Magleby K L 1999 Voltage-induced membrane displacement in patch pipettes activates mechanosensitive channels *Proc. Natl Acad. Sci. USA* **96** 14594–9
[39] Lasic D D and Needham D 1995 The stealth liposome: a prototypical biomaterial *Chem. Rev.* **95** 2601–28
[40] Needham D and Dewhirst M W 2001 The development and testing of a new temperature-sensitive drug delivery system for the treatment of solid tumors *Adv. Drug Deliv. Rev.* **53** 285–305
[41] Funakoshi K, Suzuki H and Takeuchi S 2006 Lipid bilayer formation by contacting monolayers in a microfluidic device for membrane protein analysis *Anal. Chem.* **78** 8169–74
[42] Hwang W L, Holden M A, White S and Bayley H 2007 Electrical behavior of droplet interface bilayer networks: experimental analysis and modeling *J. Am. Chem. Soc.* **129** 11854–64
[43] Needham D and Haydon D A 1983 Tensions and free energies of formation of solventless lipid bilayers. Measurement of high contact angles *Biophys. J.* **41** 251–7
[44] Haydon D A and Taylor J 1963 The stability and properties of bimolecular lipid leaflets in aqueous solutions *J. Theor. Biol.* **4** 281–96
[45] Haydon D A and Taylor J L 1968 Contact angles for thin lipid films and the determination of London–van der Waals forces *Nature* **217** 739–40
[46] White S H 1970 A study of lipid bilayer membrane stability using precise measurements of specific capacitance *Biophys. J.* **10** 1127–48
[47] White S H and Thompson T E 1973 Capacitance, area, and thickness variations in thin lipid films *Biochim. Biophys. Acta—Biomembr.* **323** 7–22
[48] Requena J and Haydon D A 1975 The lippmann equation and the characterization of black lipid films *J. Colloid Interface Sci.* **51** 315–27
[49] White S H 1978 Formation of solvent-free black lipid bilayer membranes from glyceryl monooleate dispersed in squalene *Biophys. J.* **23** 337–47
[50] Tien H T and Ottova A L 2001 The lipid bilayer concept and its experimental realization: from soap bubbles, kitchen sink, to bilayer lipid membranes *J. Membr. Sci.* **189** 83–117
[51] Baba T, Toshima Y, Minamikawa H, Hato M, Suzuki K and Kamo N 1999 Formation and characterization of planar lipid bilayer membranes from synthetic phytanyl–chained glycolipids *Biochim. Biophys. Acta—Biomembr.* **1421** 91–102
[52] Punnamaraju S and Steckl A J 2010 Voltage control of droplet interface bilayer lipid membrane dimensions *Langmuir* **27** 618–26
[53] Kresak S, Hianik T and Naumann R L C 2009 Giga-seal solvent-free bilayer lipid membranes: from single nanopores to nanopore arrays *Soft Matter* **5** 4021–32
[54] Hladky S B and Haydon D A 1972 Ion transfer across lipid membranes in the presence of gramicidin a: I. studies of the unit conductance channel *Biochim. Biophys. Acta—Biomembr.* **274** 294–312
[55] Andersen O S 1983 Ion movement through gramicidin a channels. Single-channel measurements at very high potentials *Biophys. J.* **41** 119–33

[56] Shimomura O and Johnson F H 1969 Properties of the bioluminescent protein aequorin *Biochemistry* **8** 3991–7
[57] Shimomura O 1995 A short story of aequorin *Biol. Bull.* **189** 1–5
[58] Chiesa A, Rapizzi E, Tosello V, Pinton P, de Virgilio M, Fogarty K E and Rizzuto R 2001 Recombinant aequorin and green fluorescent protein as valuable tools in the study of cell signalling *Biochem. J.* **355** 1–12
[59] Shimomura O 1995 Luminescence of aequorin is triggered by the binding of two calcium ions *Biochem. Biophys. Res. Commun.* **211** 359–63
[60] Boheim G 1974 Statistical analysis of alamethicin channels in black lipid membranes *J. Membr. Biol.* **19** 277–303
[61] Vodyanoy I, Hall J E and Balasubramanian T M 1983 Alamethicin-induced current–voltage curve asymmetry in lipid bilayers *Biophys. J.* **42** 71–82
[62] Bechinger B 1997 Structure and functions of channel-forming peptides: magainins, cecropins, melittin and alamethicin *J. Membr. Biol.* **156** 197–211
[63] Sarles S A, Bavarsad P G and Leo D J Incorporation and characterization of biological molecules in droplet–interface bilayer networks for novel active systems *Proc. SPIE* **7288** 72880H
[64] Peppas N, Hilt J, Khademhosseini A and Langer R 2006 Hydrogels in biology and medicine: from molecular principles to bionanotechnology *Adv. Mater.* **18** 1345–60
[65] Peppas N A, Keys K B, Torres-Lugo M and Lowman A M 1999 Poly(ethylene glycol)-containing hydrogels in drug delivery *J. Control. Release* **62** 81–7
[66] Tamai T, Chigane M, Matsukawa K, Ishikawa M and Inoue H 2002 Electrochromism of nickel oxide thin film with polymer gel electrolyte *J. Appl. Polym. Sci.* **83** 1305–8
[67] Ingans O, Johansson T and Ghosh S 2001 Phase engineering for enhanced electrochromism in conjugated polymers *Electrochim. Acta* **46** 2031–4
[68] Ueno K, Matsubara K, Watanabe M and Takeoka Y 2007 An electro- and thermochromic hydrogel as a full-color indicator *Adv. Mater.* **19** 2807–12